Efficient CO_2 electroreduction on tin modified cuprous oxide synthesized via a one-pot microwave-assisted route

Juqin Zeng [*1], Marco Fontana [1], Micaela Castellino [2], Adriano Sacco [1], M.Amin Farkhondehfal [1], Filippo Drago [3] and Candido Fabrizio Pirri [1,2]

[1]Center for Sustainable Future Technologies @POLITO, Istituto Italiano di Tecnologia, Via Livorno 60, 10144 Turin, Italy

[2]Department of Applied Science and Technology, Politecnico di Torino, C.so Duca degli Abruzzi 24, 10129 Turin, Italy

[3]NanoChemistry, Istituto Italiano di Tecnologia, via Morego 30, 16163 Genoa, Italy

[*]Correspondence: juqin.zeng@iit.it

Keywords: Carbon dioxide conversion; electrocatalysis; cuprous oxide; tin; overpotential

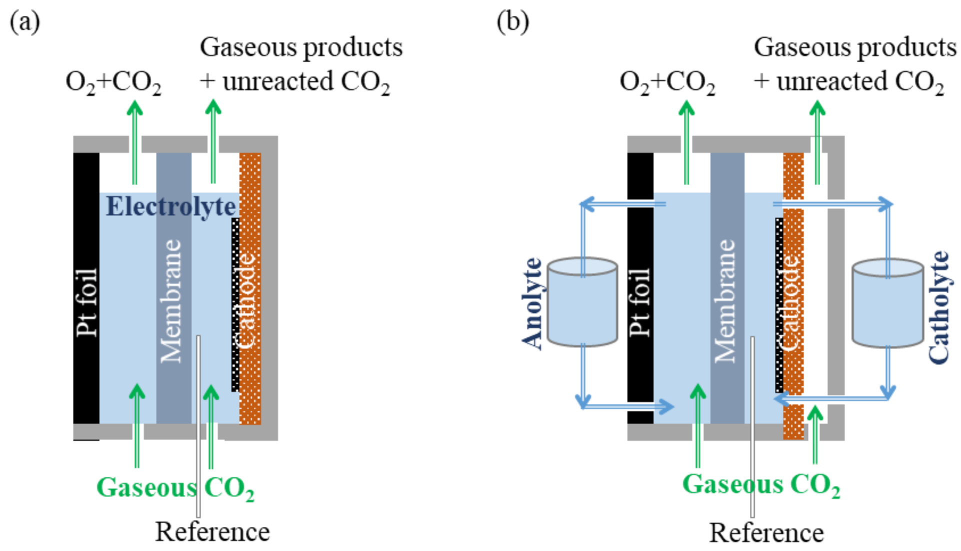

Scheme S1. Electrochemical cells for the CO_2 electrolysis: (a) batch cell and (b) semi-flow cell

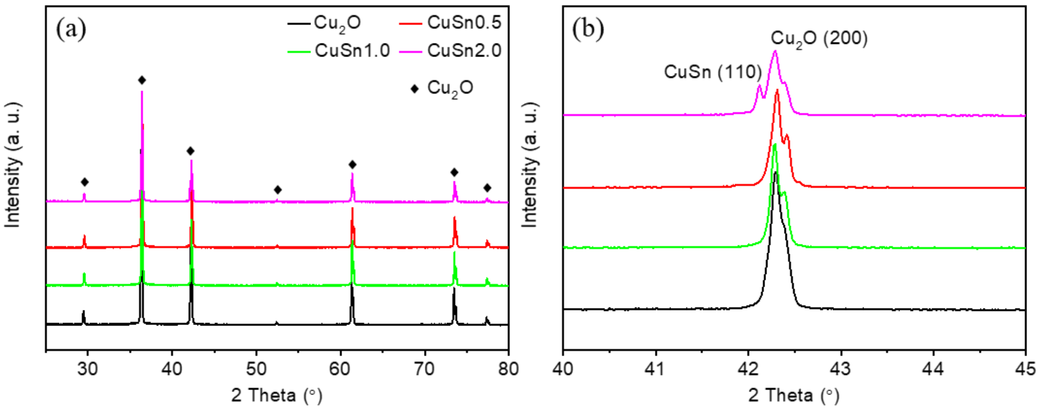

Figure S1. XRD patterns of Cu_2O, CuSn0.5, CuSn1.0 and CuSn2.0 samples (a) and a view of (200) peak (b).

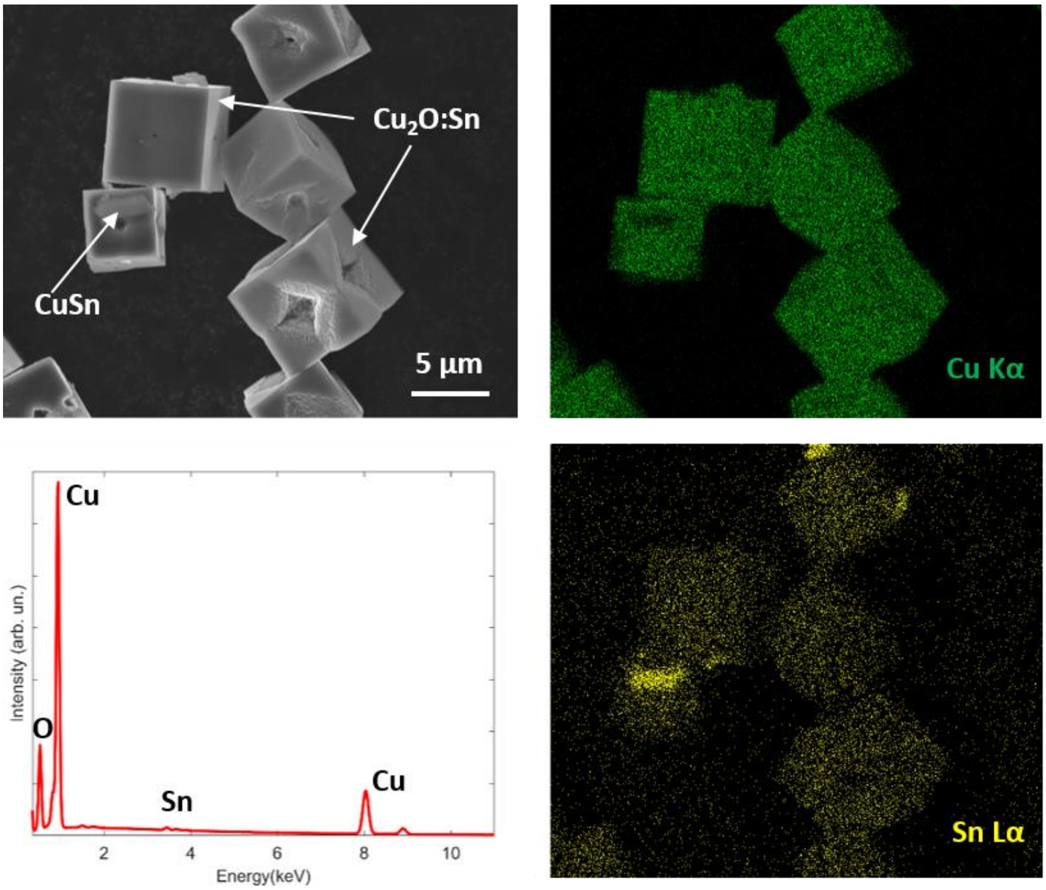

Figure S2. EDX characterization of the region of sample Sn-Cu_2O depicted in the FESEM image, consisting of an EDX spectrum, Cu Kα and Sn Lα elemental maps.

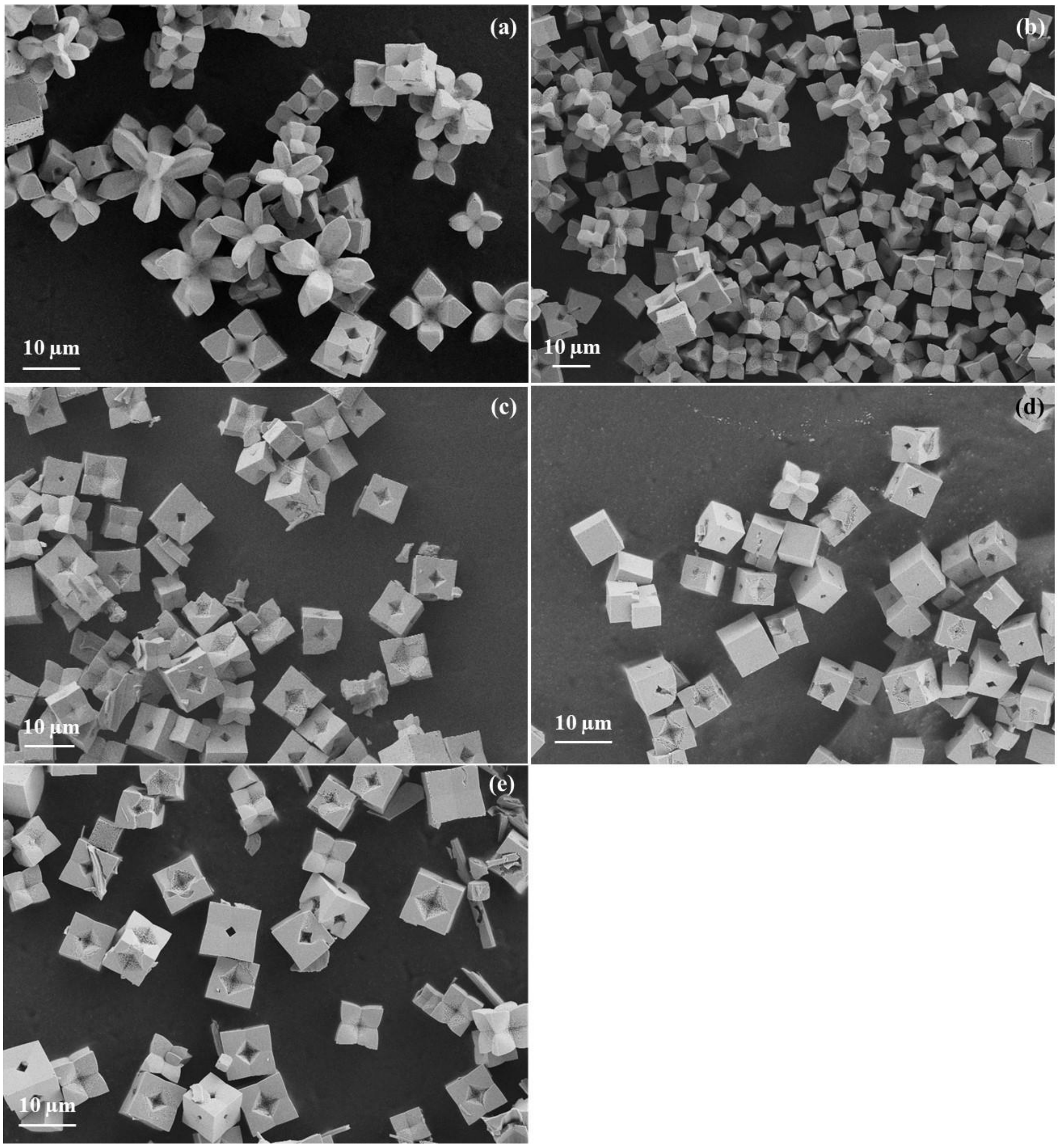

Figure S3. FESEM images of the samples. (a) Cu_2O, (b) CuSn0.5, (c) CuSn1.0, (d) Sn-Cu_2O and (e) CuSn2.0.

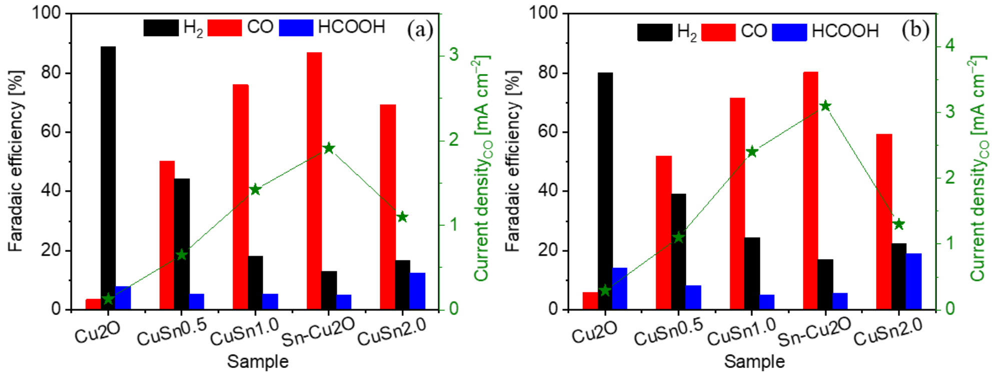

Figure S4. CO_2RR in a batch cell in a CO_2-saturated 0.1 M $KHCO_3$ aqueous solution on various samples. The dark green line is a guide to the eye for CO partial current density.

Table S1. Current density for CO formation on the Sn-Cu_2O electrode at various potentials in different electrolytes.

Electrolyte ($KHCO_3$)	**0.1 M**	**0.5 M**	**1.0 M**	**2.0 M**
Potential (V vs. RHE)	Current density$_{CO}$ (mA cm^{-2})	Current density$_{CO}$ (mA cm^{-2})	Current density$_{CO}$ (mA cm^{-2})	Current density$_{CO}$ (mA cm^{-2})
-0.35	0.097	0.14	0.28	0.36
-0.4	0.25	0.33	0.47	0.68
-0.45	0.52	0.73	0.88	0.98
-0.5	0.78	1.37	1.82	1.88
-0.55	1.27	2.03	2.61	3.36
-0.6	1.76	3.88	5.45	6.23
-0.7	3.17	5.95	11.25	12.28
-0.8	4.87	9.09	16.73	24.40
-0.9	9.90	14.80	22.66	36.38
-1.0	13.87	22.00	29.30	47.16

Table S2. Faradaic efficiency for CO formation on the Sn-Cu_2O electrode at various potentials in different electrolytes.

Electrolyte ($KHCO_3$)	**0.1 M**	**0.5 M**	**1.0 M**	**2.0 M**
Potential (V vs. RHE)	FE_{CO} (%)	FE_{CO} (%)	FE_{CO} (%)	FE_{CO} (%)
-0.35	45	42	72	51
-0.4	56	58	79	55
-0.45	79	70	81	64
-0.5	84	78	81	70
-0.55	85	85	83	74
-0.6	90	87	86	75
-0.7	90	90	83	79
-0.8	90	89	80	76
-0.9	82	88	76	71
-1.0	80	83	73	68

Table S3. Comparison of different CuSn-based electrocatalysts in liquid-phase CO_2 electrolysis.

Electrocatalyst	Potential (V vs RHE)	Electrolyte	j_{CO} (mA cm^{-2})	FE_{CO} (%)	Reference
Electrodeposited Cu-Sn	-0.6	0.1 M $KHCO_3$	0.9	90	1
Dendritic Cu-Sn	-0.8	0.1 M $KHCO_3$	4.7	90	2
Electrodeposited Cu-Sn	-0.99	0.1 M $KHCO_3$	0.9	60	3
Dendritic Cu-Sn	-1.1	0.1 M $KHCO_3$	11.5	75	4
3D-hierarchical Cu-Sn	-1.0	0.1 M $KHCO_3$	9.6	≈70	5
Cu/patterned-Sn	-1.0	0.1 M $KHCO_3$	1.9	58	6
Core/Shell Cu/SnO_2	-0.7	0.5 M $KHCO_3$	≈4.3	93	7
Sn/Cu-Nanofiber-GDE	-1.2	0.1 M $KHCO_3$	100	≈80	8
Sn-Cu_2O	-1.0	2.0 M $KHCO_3$	47	70	This work
Sn-Cu_2O	-0.7	0.5 M $KHCO_3$	5.9	90	This work

References

1. Sarfraz, S.; Garcia-Esparza, A.T.; Jedidi, A.; Cavallo, L.; Takanabe, K. Cu-Sn Bimetallic Catalyst for Selective Aqueous Electroreduction of CO_2 to CO. *ACS Catal.* **2016**, *6*, 2842-2851.

2. Zeng, J.; Bejtka, K.; Ju, W.; Castellino, M.; Chiodoni, A.; Sacco, A.; Farkhondehfal, M.A.; Hernández, S.; Rentsch, D.; Battaglia, C.; Pirri, C.F. Advanced Cu-Sn foam for selectively converting CO2 to CO in aqueous solution. *Appl. Catal. B Environ.* **2018**, *236*, 475-482.

3. Morimoto, M.; Takatsuji, Y.; Yamasaki, R.; Hashimoto, H.; Nakata, I.; Sakakura, T.; Haruyama, T. Electrodeposited Cu-Sn Alloy for Electrochemical CO_2 Reduction to CO/$HCOO^-$. *Electrocatalysis*, **2018**, *9*, 323-332.

4. Ju, W.; Zeng, J.; Bejtka, K.; Ma, H.; Rentsch, D.; Castellino, M.; Sacco, A.; Pirri, C.F.; Battaglia, C. Sn-Decorated Cu for Selective Electrochemical CO_2 to CO Conversion: Precision Architecture beyond Composition Design. *ACS Appl. Energy Mater.* **2019**, *2*(1), 867-872.

5. Yoo, C.J.; Dong, W.J.; Park, J.Y.; Lim, J.W.; Kim, S.; Choi, K.S.; Ngome, F.O.O.; Choi, S.-Y.; Lee, J.-L. Compositional and Geometrical Effects of Bimetallic Cu–Sn Catalysts on Selective Electrochemical CO_2 Reduction to CO. *ACS Appl. Energy Mater.* **2020**, *3*, 4466-4473.

6. Dong, W.J.; Lim, J.W.; Hong, D.M.; Park, J.Y.; Cho, W.S.; Baek, S.; Yoo, C.J.; Kin, W.; Lee, J.-L. Evidence of Local Corrosion of Bimetallic Cu-Sn Catalysts and Its Effects on the Selectivity of Electrochemical CO_2 Reduction. *ACS Appl. Energy Mater.* **2020**, *3*, 10568-10577.

7. Li, Q.; Fu, J.; Zhu, W.; Chen, Z.; Shen, B.; Wu, L.; Xi, Z.; Wang,T.; Lu, G.; Zhu, J.J.; Sun, S. Tuning Sn-Catalysis for Electrochemical Reduction of CO_2 to CO via the Core/Shell Cu/SnO_2 Structure. *J. Am. Chem. Soc.* **2017**, *139*, 4290-4293.

8. Ju, W.; Jiang, F.; Ma, H.; Pan, Z.; Zhao, Y.-B.; Pagani, F.; Rentsch, D.; Wang, J.; Battaglia, C. Electrocatalytic Reduction of Gaseous CO_2 to CO on Sn/Cu-Nanofiber-Based Gas Diffusion Electrodes. *Adv. Energy Mater.* **2019**, *9*, 1901514.